Geol. Mag. **140** (2), 2003, pp. 157–172. © 2003 Cambridge University Press
DOI: 10.1017/S0016756803007283 *Printed in the United Kingdom*

Brittle fault evolution of the Montréal area (St Lawrence Lowlands, Canada): rift-related structural inheritance and tectonism approached by palaeostress analysis

MURIEL ROCHER*‡, ALAIN TREMBLAY*, DENIS LAVOIE§ & ANDRÉ CAMPEAU¶

*INRS-Géoressources, Québec Geoscience Centre, 880 Ch. Ste-Foy, CP 7500, Ste-Foy, Québec G1V 4C7, Canada
§Geological Survey of Canada, 880 Ch. Ste-Foy, CP 7500, Ste-Foy, Québec G1V 4C7, Canada
¶Service de Travaux Publics, Division de la Voirie, 999 Louvain Est, Montréal, Québec M2M 1B3, Canada

(*Received* 12 February 2002; *revised version received* 20 June 2002; *accepted* 2 December 2002)

Abstract – The Montréal area belongs to the St Lawrence Lowlands, a Cambrian Early Ordovician passive margin of the Iapetus Ocean, later covered by Appalachian Middle to Upper Ordovician foreland deposits. A structural and palaeostress analysis has been carried out in order to reconstruct its tectonic evolution. The structural map has been revised with new data. Palaeostresses are reconstructed based on inversion of fault slip data, and these results are independently corroborated by the microstructural study of calcite mechanical twinning. Field relationships are used to establish the relative chronology of fractures and to deduce the motion on regional faults. The reconstructed structural and tectonic evolution brings to light some relationships between structural inheritance and tectonic events that have affected the area since Early Palaeozoic times. An early NW–SE extension is responsible for N040-trending faults along the northern border of the St Lawrence Lowlands, and for N090- and N120-trending faults cross-cutting the Montréal area. This extension is followed by WNW–ESE and NNW compressions, which have induced reverse motion on pre-existing faults and generated strike-slip conjugate faults. Subsequent NE–SW and NNW–SSE-directed extensions have reactivated previous faults with normal to strike-slip motions. A late NE–SW compression is recorded in the Monteregian plutons. Compressions in WNW–ESE and NNW directions are consistent with Appalachian collisional tectonism, but N040- and N090-trending faults cross-cut Appalachian folds and foreland deposits. Although the early NW–SE extension is consistent with the collapse of the Iapetan margin in Early Palaeozoic times, most of the present geometry of the St Lawrence Lowlands could be attributed to Mesozoic tectonism, recorded as nearly N–S-directed extensional events.

Keywords: stress fields., rifting, structural analysis, Montréal, Québec.

1. Introduction

The Montréal area of southern Québec (Fig. 1a,b) is part of the central St Lawrence Lowlands platform (Sandford, 1993), a slightly deformed Cambrian to Early Ordovician passive continental margin succession (L. Bernstein, unpub. Ph.D. thesis, Univ. Montréal, Canada, 1991; Salad Hersi & Lavoie, 2000*a*, *b*), overlain by Middle to Late Ordovician shallow to deep marine foreland basin deposits (Lavoie, 1994). In southern Québec, the St Lawrence Lowlands are separated to the southeast from the Palaeozoic Appalachian belt by faults related to Logan's Line, and to the northwest from the Proterozoic Grenville province by either an angular unconformity or nearly N040-trending faults (Fig. 1b).

The stratigraphic and structural geology of the Montréal area is mainly based on fieldwork by Clark (1940, 1941, 1947), later synthesized by Clark (1972), who depicted several sets of brittle faults trending N090, N040 and N140 (Fig. 2e) cross-cutting the St Lawrence Lowlands rock units. N040- and N090-trending faults appear to be characterized by a significant amount of vertical offset (tens to hundreds of metres), but the age of faulting has been debated (e.g. Kumarapeli & Saull, 1966; Glasmacher, Tremblay & Zentilly, 1998). The structural history of the St Lawrence Lowlands began in Late Precambrian–Early Cambrian times with intracontinental rifting that resulted in the formation of the Iapetus Ocean (Sandford, 1993). Magmatic rocks associated with this event (Late Precambrian–Early Cambrian dykes, plutons and carbonatites: e.g. Kumarapeli & Saull, 1966) occur along both the St Lawrence and the Ottawa–Bonnechère grabens (Fig. 1a), with a triple junction located in the vicinity of the Montréal area (Fig. 1a,b). Rifting along the St Lawrence graben left a failed arm (aulacogene) along the Ottawa–Bonnechère graben (Kumarapeli, 1985). Gradual marine transgression over the Grenvillian basement led to the deposition of an initial siliciclastic succession (Cambrian–Potsdam Group) followed by a shallow marine carbonate (Early Ordovician–Beekmantown Group) passive margin

‡ Author for correspondence: muriel.rocher@irsn.fr;
Present address: 9 av. de la Malibran, F-77680 Roissy-en-Brie, France.

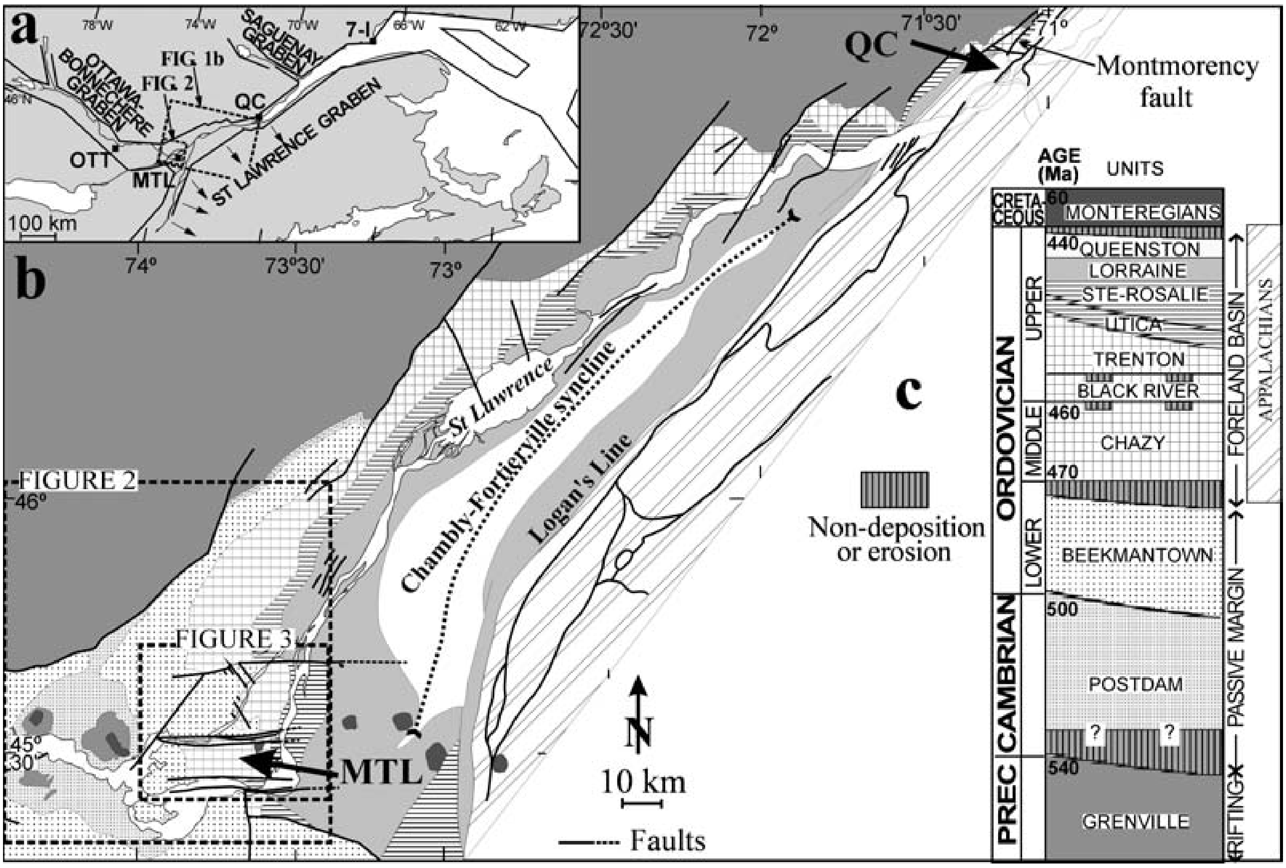

Figure 1. Regional setting. (a) The St Lawrence and Ottawa–Bonnechère River grabens and fault boundaries after Kumarapeli & Saull (1966). Arrows indicate direction of opening of Iapetus Ocean. QC: Québec city; MTL: Montréal, OTT: Ottawa, 7I: Sept-Iles. (b) Geological map of the St Lawrence Lowlands (from Globensky, 1987). For legend see (c). (c) Stratigraphic framework for the Palaeozoic succession of the St Lawrence Lowlands (modified from Lavoie, 1994).

succession. In Middle Ordovician times, subduction led to the development of a foreland basin that developed during Appalachian orogenies which, in southern Québec, correspond to the Late Ordovician Taconian orogeny and the Devonian Acadian orogeny (Sandford, 1993). These events variously affected the St Lawrence Lowlands platform in the Montréal area. Open folds developed in the area, such as the Chambly–Fortierville syncline (Fig. 1b), are currently attributed to the Taconian and/or Acadian orogenies (Williams, 1979). Following the formation of the Appalachian orogen, rifting of the Atlantic Ocean–Labrador Sea during Mesozoic times possibly reactivated pre-existing faults (e.g. Kumarapeli & Saull, 1966; Carignan, Gariépi & Hillaire-Marcel, 1997), and was almost coeval with the emplacement of igneous rocks of the Monteregian Hills in Early Cretaceous times (Foland *et al*. 1986; McHone & Butler, 1984; Pe-Piper & Jansa, 1987). According to Zoback *et al*. (1986), the area has been in a compressive crustal stress state since the Tertiary as the North Atlantic spreading ridge has pushed on the North American Plate.

Since Clark's comprehensive summary (1972), a large amount of detailed stratigraphic and structural data has been collected in the Montréal area following (1) the availability of quarries and roadcuts along new highways, (2) subway development, and (3) drilling for the construction of a regional water treatment plan. All these new data (see Section 3) were used to revise the existing geological map, and to improve our knowledge of the nature and geometry of regional faults. Our work concerns the analysis of the kinematics and the origin of brittle faults in order to propose a structural and tectonic evolution for the St Lawrence Lowlands in the Montréal area since Palaeozoic times. The area has undergone a complete Wilson cycle (Wilson, 1966), from Precambrian rifting to Appalachian compressive deformation followed by renewed crustal stretching, most likely related to rifting of the Atlantic Ocean in Mesozoic times. A more specific aspect of the study is to discuss the effects of structural inheritance on the morphology of the Appalachian foreland basin and on the Mesozoic rifting event. However, this region displays low topography with few natural outcrops, and most structures have to be characterized through other types of geoscience information (see Section 3), and the relative motion of faults has been mainly deduced from palaeostress reconstruction.

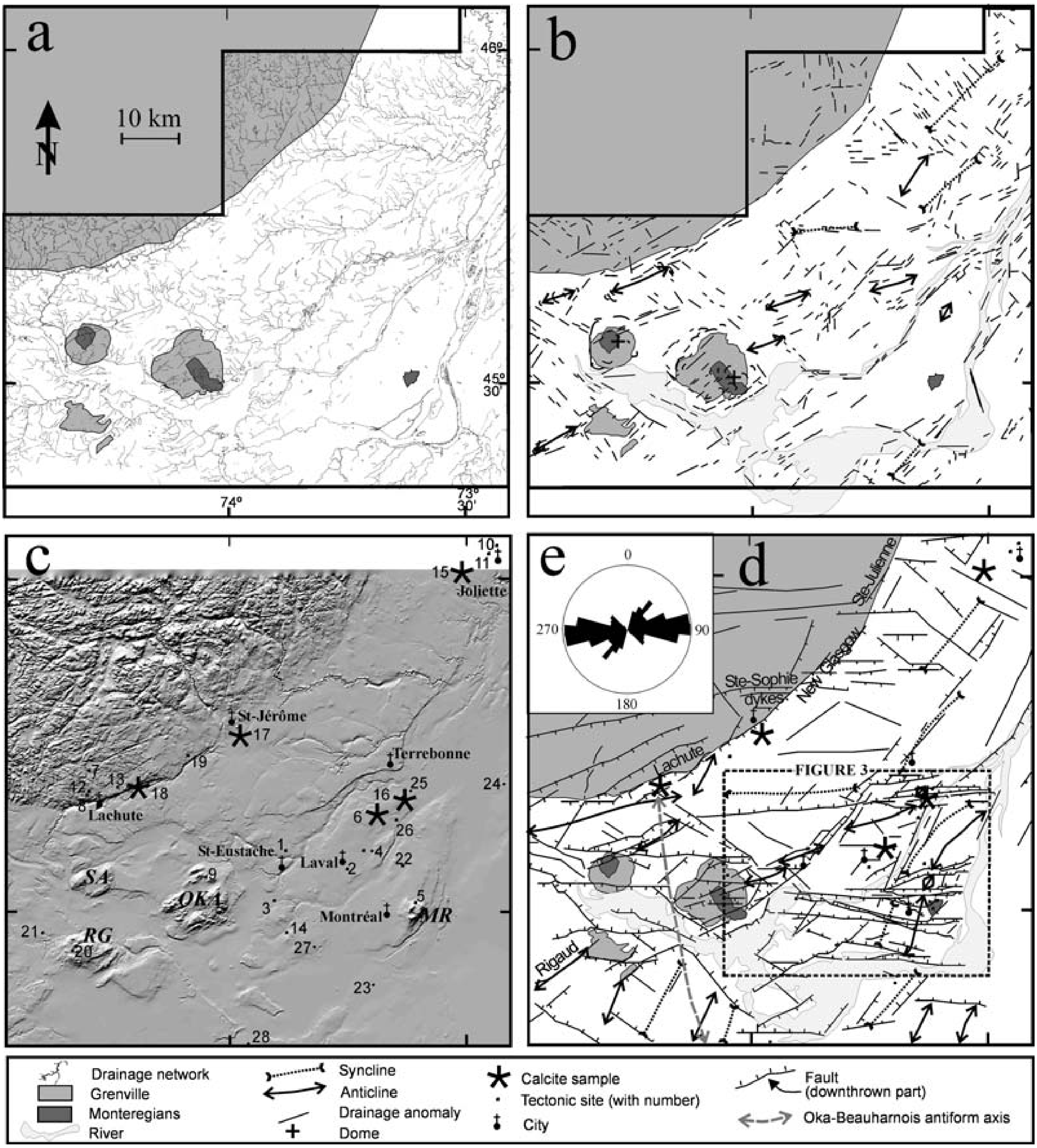

Figure 2. (a) Drainage network extracted from 1 : 25 000 topographic maps and completed with temporary watercourses and backwater deduced from topography. (b) Rectilinear and curvilinear anomalies of drainage network. (c) Digital Elevation Model. Sites (quarries and natural exposures) 1–16: structural observations and fault slip analysis; 17–22: structural observations; 23–28: fault slip analysis by Faure (S. Faure, unpub. Ph.D. thesis, Univ. du Québec, 1995). OKA: Oka hill, SA: Saint-André hill, MR: Mont Royal, RG: Mont Rigaud. (d) Structural map of the St Lawrence Lowlands in southwestern Québec, based on surface (drainage network anomalies, DEM, fieldwork) and drilling data, modified from Clark (1972). (e) Rose diagram showing frequency of measured fault trends.

2. Geological setting

In the Montréal area, the St Lawrence Lowlands correspond to a siliciclastic and carbonate platform having a maximum thickness of 1200 metres, overlain by approximately 1800 metres of foreland deposits (Fig. 1b,c) (Sandford, 1993; Lavoie, 1994).

The base of the platformal sequence consists of the Cambrian Potsdam Group, fluvial to shallow marine siliciclastic deposits unconformably overlying the Precambrian basement (Salad Hersi & Lavoie, 2000*a*,*b*). The Potsdam Group is overlain by the Beekmantown Group, a Lower Ordovician carbonate platform marking the final phase of passive margin sedimentation, and consisting of three stratigraphic units, the Theresa, Beauharnois and Carillon formations (L. Bernstein, unpub. Ph.D. thesis, Univ. Montréal, Canada, 1991). The top of the Beekmantown Group is characterized by a major erosional unconformity (Sauk-Tippecanoe unconformity: Sloss, 1988) that marks the end of passive margin sedimentation and a significant marine relative sea-level fall likely related to the migration of a tectonic flexural bulge along the margin (Knight, James & Lane, 1991).

The overlying sequence of foreland basin carbonates comprises the Chazy, Black River and Trenton groups (Fig. 1c). Salad Hersi & Dix (1999) and Lavoie (1994, 1995) attribute local marine regressions between the Chazy and the Black River groups and between the Black River and the Trenton groups to faulting due to irregular Appalachian tectonic pulses. Regional facies distribution and thickness variations within the Trenton Group have been attributed to syn-sedimentary normal block faulting (Lavoie, 1994, 1995). The top of the Trenton Group consists of muddy limestone beds with abundant interbeds of shales. The increasing proportion of shale heralds the overlying regressive flysch to molasse sequence that is made up of the Utica, Sainte-Rosalie, Lorraine and Queenston groups (Fig. 1c), commonly seen as marking the erosion of Appalachian nappes adjacent to the St Lawrence Lowlands.

There are two types of igneous rocks in the St Lawrence Lowlands in the Montréal and Ottawa areas, (1) Late Precambrian–Early Cambrian intrusions attributed to Iapetan rift magmatism forming dykes (e.g. Ste-Sophie dykes, Fig. 2d, 520 Ma: Doig & Barton, 1968; or along the Ottawa–Bonnechère graben, Fig. 1a, 545 Ma: Kamo & Krogh, 1995), high-level felsic plutons (e.g. Mont Rigaud, Fig. 2c, 564 Ma: E. Malka, unpub. Mémoire U. Q. A. M., Québec, 1997) and carbonatites (e.g. Manitou Islands, west of the city of Ottawa, 565 Ma: Gittins, McIntyre & York, 1967), and (2) Early Cretaceous intrusions of the Monteregian series (*c*. 125 Ma: Foland *et al*. 1986), such as the Mont Royal, and the Oka and Saint-André hills (Fig. 2c).

3. Structural geology of the Montréal area

Several thousand shallow wells reaching bedrock were drilled during the development of subway lines and water collectors within and around the city of Montréal (Fig. 3a, data from Public Works Service of Montréal). These wells (nearly 40 metres depth in the bedrock) provide lithological information and some structural data, and their close spacing provides information about fault offsets. Structural mapping of subway galleries (lines 2 and 5), and the description of rock units crossed during the subway construction were also available for our study (Fig. 3a). We also used a thickness map of Quaternary deposits of the area (Ross *et al*. 2001). These variations of thickness can be attributed to both the erosion related to the last glaciations, and significant pre-Quaternary palaeotopography suggesting active faulting. We have also made structural observations in quarries and natural exposures of the area (Fig. 3a). These data allowed us to revise the geological map of the Montréal and Jésus islands, as shown on Figure 3b.

The Montréal area occupies the western flank of the Chambly–Fortierville syncline (Fig. 1b), and the bedding is commonly gently dipping ($\sim 5°$) eastward. Minor folds (e.g. Ile Jésus and Villeray anticlines, Ahuntsic and Sainte-Thérèse synclines; Fig. 3b) trend NNE–SSW and are interpreted as structures related to the Chambly–Fortierville syncline. Existing geological maps (Clark, 1972; Globensky, 1987), field mapping, drainage network patterns and topographic analysis were compiled to propose a regional revised structural map of the Montréal area (Fig. 2). In flat regions such as the Montréal area, where bedrock exposure is scarce, the analysis of hydrographic network and topography is useful for structural mapping. Drainage pattern studies contribute significantly to structural analyses (e.g. Deffontaines & Chorowicz, 1991), even in areas where bedrock structures are buried (Scanvic, 1983). For our study, we transferred the drainage network extracted from the 1 : 25 000 topographic maps of the Montréal area, along with temporary watercourses and backwater deduced from topography (Fig. 2a), and we identified a series of rectilinear and curvilinear drainage patterns (Fig. 2b). Anticlines and synclines commonly generate peculiar drainage networks (Deffontaines, 1990), including annular and curvilinear patterns on their periclinal terminations. Faults and lithological variations generate rectilinear drainage patterns. The analysis of topographic relief by Digital Elevation Modelling (Fig. 2c) has also been useful for our structural analysis. Faults trending N090, N120 and N040, frequently marked by drainage patterns (Fig. 2b), are present and cross-cut the regional fold axes. These faults are subvertical (except faults with reverse motion), alternatively show ‘pseudotachylyte’ veins or cataclastic breccias, and are marked by closely spaced unfilled joints. Vertical fault offsets have been locally determined from the displacement of lithological markers between closely spaced (tens of metres) drilling wells.

3.a. Montréal and Jésus islands

For Montréal and Jésus islands (Fig. 3b), the compilation of these data is consistent with the existence of major N090-trending faults as mapped by Clark (1972), and their location has been precisely determined (within 50 m). Three major fault zones are recognized,

https://doi.org/10.1017/S0016756803007283 Published online by Cambridge University Press

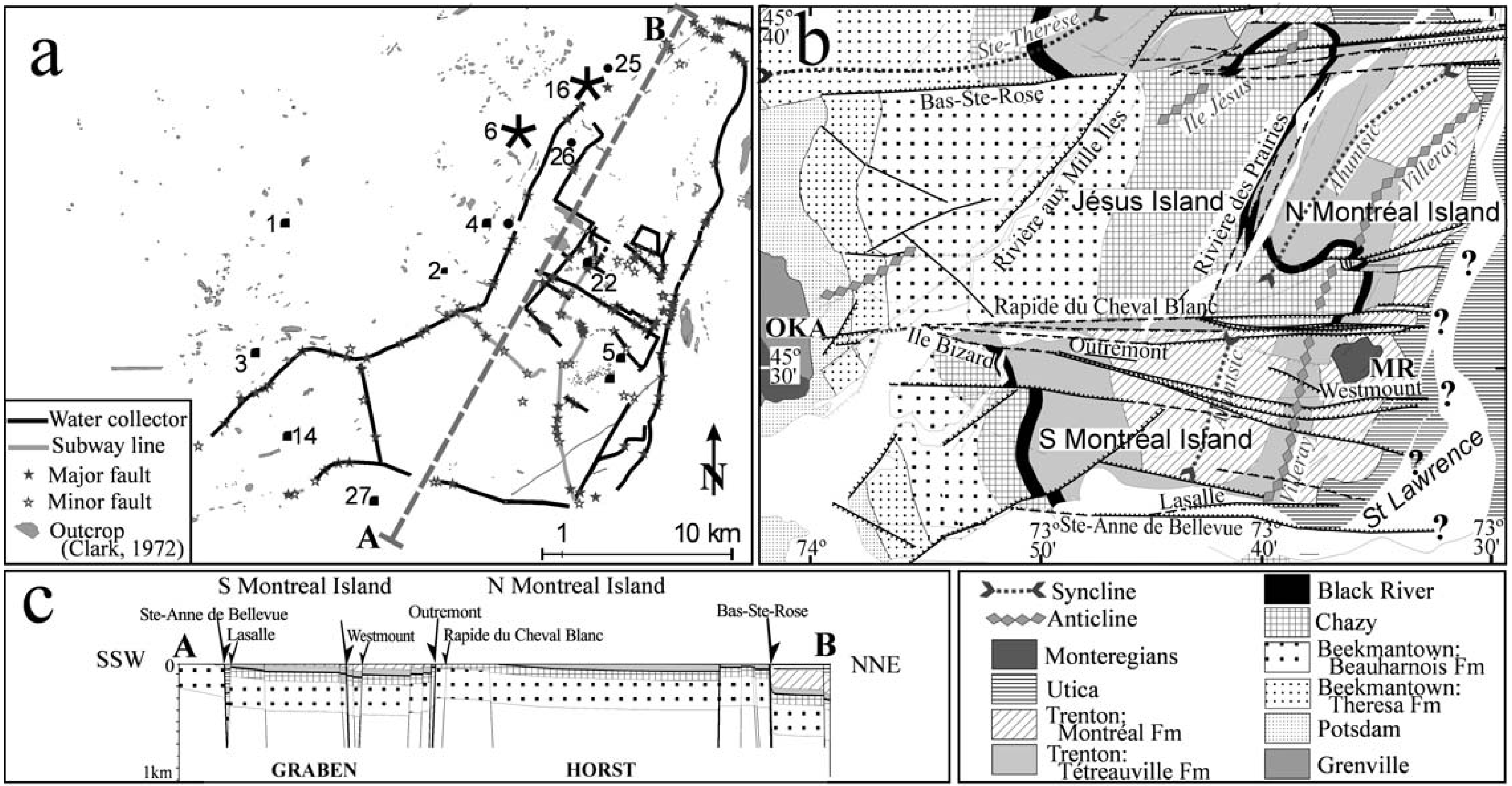

Figure 3. (a) Sites of structural and tectonic field observations (see Fig. 2 legend and caption), and data (faults) from Public Works Service of Montréal, acquired during the development of subway lines (structural and lithological maps of galleries) and water collectors (wells every 50 metres) on Montréal Island. (b) Geological map of Montréal Island, modified from Clark (1972). (c) NNE–SSW cross-section of Montréal Island, constructed with subsurface data of Figure 3a.

from north to south: the Bas-Sainte-Rose, Rapide-du-Cheval-Blanc, and Sainte-Anne-de-Bellevue fault zones (names after Clark, 1972) (Fig. 3b). These faults clearly cross-cut folds with axes trending NNE–SSW that we attributed to the Chambly–Fortierville syncline system. As an example, the Rapide-du-Cheval-Blanc fault zone cross-cuts the Villeray anticline and the Ahuntsic syncline (Fig. 3b,c), which explains why the Chazy rocks (northern side) are in contact with the Tétreauville Formation of Trenton Group (southern side) along the Ahuntsic syncline axis. The Rapide-du-Cheval-Blanc fault zone consists of a series of steeply S-dipping normal faults (the Ile-Bizard, the Rapide-du-Cheval-Blanc and Outremont faults; Fig. 3b) with a total vertical offset of *c.* 100 m (Fig. 3c). Westward, faults trending N040 of the Rivière-aux-Mille-Iles fault zone (Fig. 3b) slightly cross-cut structures related to the Rapide-du-Cheval-Blanc fault zone. The Bas-Sainte-Rose fault zone forms the northernmost series of N090-trending faults in the Montréal area. It dips very steeply toward the north and displays a vertical displacement of *c.* 200 m (Fig. 3c) with nearly 3 km of apparent left-lateral offset (Fig. 3b). The Bas-Sainte-Rose fault zone extends westward (with decreasing apparent vertical and lateral offsets) and apparently cross-cuts the Rivière-aux-Mille-Iles fault zone (Fig. 3b). In the southern part of Montréal Island, the Sainte-Anne-de-Bellevue fault zone (Fig. 3b) dips toward the north. Although we interpret it as a normal fault with left-lateral strike-slip component, its vertical offset has not been precisely determined. At the scale of Montréal and Jésus islands, N090-trending fault zones define a succession of horsts and grabens, main horsts occurring on Jésus Island and on the northern part of Montréal Island, and the graben structure being located in the southern part of Montréal Island (Fig. 3c).

The folds are not only cross-cut and shifted by the N090-trending Bas Sainte-Rose fault, but the axes are also progressively turned in its vicinity, tending to become parallel to the fault. It is also the case for some other N090-trending faults. This could indicate an important strike-slip motion of the fault during folding.

Minor N140-trending faults previously mapped by Clark (1972) along the western limit of Montréal Island were not observed during this study, but we recognized N020-trending faults in the same area, here referred to as the Rivière-des-Prairies fault zone (see Fig. 3b). These faults probably belong to the same generation of faults as those of the Rivière-aux-Mille-Iles system, and possibly as those of the northwestern border of the basin.

3.b. Montréal area

At the scale of the Montréal area, regional faults are trending N090, N020 to N040 and N120 (Fig. 2e). The principal structural characteristics of the revised map are follows:

(1) N090-trending fault zones of Montréal and Jésus islands (Fig. 3b) are laterally continuous, however, the Rapide-du-Cheval-Blanc fault zone becomes less important to the west. Fault offset is on the scale of metres in the Saint-André and Oka intrusions (Figs 2d,3b).

(2) North and northwest of Montréal (Fig. 2c,d), N090-trending faults affect both the Grenvillian basement and the St Lawrence Lowlands platform.

(3) Clark (1972) has mapped the Lachute fault along the northern border fault of the St Lawrence Lowlands. We also observed a N090-trending fault in the vicinity of the town of Lachute, as well as a discontinuous zone of N040-trending faults (New Glasgow and Sainte-Julienne faults) to the northeast (Fig. 2d).

(4) N020 to N040-trending faults of the Montréal city area, such as the Rivière-aux-Mille-Iles and Rivière-des-Prairies faults, extend northward and southward from this area (Fig. 3b) and affect the Mont-Royal, Saint-André and Oka intrusions.

(5) An antiform structure originally interpreted by Clark (1972) as a pre-Appalachian structure (the 'Oka-Beauharnois antiform') to explain the occurrence of Cambrian rocks in the centre of the study area (Fig. 1) is more likely the result of a series of Appalachian anticlines trending NE–SW.

In summary (Table 3), N090-trending faults of the Montréal area cross-cut folds trending NE–SW to NNE–SSW of the Chambly–Fortierville syncline system with major offsets but do not significantly affect the Oka and Saint-André Cretaceous intrusions. We conclude that major faulting along these faults post-dates the Taconian and/or Acadian orogenesis, but has pre-dated or been coeval with the Monteregian plutonism (see also McHone, 1978; Philpotts, 1974). N120-trending faults are cross-cut by N090-trending faults, suggesting that the former faulting event occurred slightly prior to N090 faulting. Faults trending nearly N040 show complex relationships with N090 faults. The N040-trending faults commonly cross-cut N090-trending faults, thus suggesting that these faults record late motions. The late motion may have occurred only along N040-trending faults. However, because both the N040- and N090-trending faults cross-cut the Monteregian plutons, fault increments post-dating Early Cretaceous times are inferred.

4. Palaeostress reconstructions

The kinematics of most regional faults could not be determined solely on the basis of direct field observations, because of the low density of bedrock exposures. Palaeostress reconstructions, using data from striated fault planes and from the analysis of calcite mechanical twinning from oriented samples, were performed in order to determine the kinematic framework of major faults formed during each of the inferred tectonic events.

The orientations of multiple sets of fractures and minor faults occurring in quarries, roadcuts and natural exposures of the Montréal area have been measured (nearly 350 fault striae, sites on Fig. 2c), and oriented calcite samples were taken where possible (six samples, Fig. 2c). Palaeostress axes were then determined using the inverse method of A. Etchecopar (unpub. Ph.D. Thesis, Univ. Montpellier, France, 1984; see Tourneret & Laurent, 1990) for analysis of calcite twins, and the method of Angelier (1984, 1990) for analysis of fault slips.

4.a. The inverse analysis of calcite twin data

At low pressure and temperature conditions, calcite aggregates deform primarily by twinning (Fig. 5) along $\{01\bar{1}2\}$ crystallographic planes called the *e*-twin planes (Turner, Griggs & Heard, 1954). Mechanical twinning of calcite crystals occurs only if the resolved shear stress acting along each *e* plane equals or exceeds the yield stress value for twinning (e.g. Tourneret & Laurent, 1990). For each sampling site of the Montréal area (Fig. 2c), calcite twin data (twinned and untwinned *e* planes) were collected using the Universal Stage with measurements made on three mutually perpendicular thin sections.

The orientation of palaeostress axes from twin data was determined through numerical inversion (A. Etchecopar, unpub. Ph.D. thesis, Univ. Montpellier, France, 1984), a technique that has been validated in various regions of unmetamorphosed and weakly deformed carbonate cover rocks (e.g. Tourneret & Laurent, 1990; Lacombe *et al*. 1990, 1996; Lacombe, Angelier & Laurent, 1992, Rocher *et al*. 1996, 2000*a*; Rocher & Tremblay, 2001). Theoretically, the value of the resolved shear stress must be larger for all the twinned planes consistent with the tensor-solution than for the untwinned planes. Data inversion then provides the orientation of principal stress axes σ_1, σ_2 and σ_3 (positive compression, $\sigma_1 \geq \sigma_2 \geq \sigma_3$) related to calcite twinning (Turner, 1953; Dietrich & Song, 1984; Pfiffner & Burkhard, 1987; Lacombe, Angelier & Laurent, 1992), and the Φ ratio ($\Phi = (\sigma_2 - \sigma_3)/(\sigma_1 - \sigma_3)$; $0 < \Phi < 1$) (Tourneret & Laurent, 1990).

In the case of a single event of tectonism, most measured twinned planes are consistent with the state of stress, and inconsistent results are considered as background noise (less than 30%, see, e.g. Tourneret & Laurent, 1990). If tectonism is polyphase, several twinned planes can be inconsistent with the first calculated stress tensor (up to 70%). In such cases, the separation of superimposed stress tensors is made by a second tensor calculation using the inconsistent twinned planes and the whole set of untwinned planes. Such an iterative method has been shown to provide consistent results for stress reconstructions from polyphase fault sets (e.g. Lacombe, Angelier & Laurent, 1992; Rocher *et al*. 2000*a*). M. Rocher (unpub. Ph.D. Thesis, Univ. Paris VI, 1999) has shown that the determination of superimposed stress tensors using Etchecopar's method (see Tourneret & Laurent, 1990) is commonly accurate, with $< 5^\circ$ of error for the orientation of principal stress axes, and < 0.1 for the Φ ratio.

4.b. The inverse analysis of fault slip data

The inverse analysis of fault slip data allows the determination of palaeostress orientations from measurements of the orientation and the dip and sense of slip of numerous minor faults (e.g. Carey & Brunier, 1974; Etchecopar, Vasseur & Daignieres, 1981; Angelier, 1984, 1990) (Fig. 4). The method is based on the assumption that the stria on a fault plane is parallel to the resolved shear stress applied on this surface.

The inversion of fault slip data yields a reduced stress tensor, including the orientation of the principal stress axes σ_1, σ_2 and σ_3 and the value of the Φ ratio. For our study, we have used the computerized methods of Angelier (1975, 1976, 1984, 1990).

In the case of polyphase faulting, mechanically consistent fault data are grouped into data subsets on the basis of relative chronological relationships such as the superposition of several striae on a single fault plane (Fig. 4), cross-cutting faults, the age of host rocks, and relationships with regional folds. Stress tensors are then calculated for each fault subset. Angelier's method yields two estimators of the error margin called α and RUP (Table 1). The α parameter ranges from 0° to 180° and represents the angle between the observed stria and the computed shear stress (low misfit below 22.5°). The RUP parameter is a value between 0 and 200 that depends on both the angle between observed and computed striae and the magnitude of shear stress (low misfit below 50) (Angelier, 1990).

Relative age information can be used to establish the chronology of faults occurring at different sites. Age information is commonly scarce in comparison to the number of measurements from a given site (Fig. 4, Table 1), and it is therefore necessary to infer age relationships established on the basis of a small number of field observations to all data collected in a site, considering, however, the mutual geometric and mechanical compatibility of datasets. Moreover, the chronology of all reconstructed events is commonly not recorded in a single site. For instance, in the Beaudry quarry of the Lachute area (site 7, Fig. 2c), we locally observed N110 striated faults (Fig. 4a) with left-lateral strike slip motion, that is, consistent with a nearly WNW compression (a compression with σ_1 trending nearly WNW–ESE) (Fig. 4b, diagram 1) that are cross-cut by normal fault striae, that is, consistent with a NE–SW extension (an extension with σ_3 trending NE–SW) (Fig. 4b, diagram 2). Relative age data obtained from several sites were thus used to infer a succession of deformational events at the regional scale, assuming

https://doi.org/10.1017/S0016756803007283 Published online by Cambridge University Press

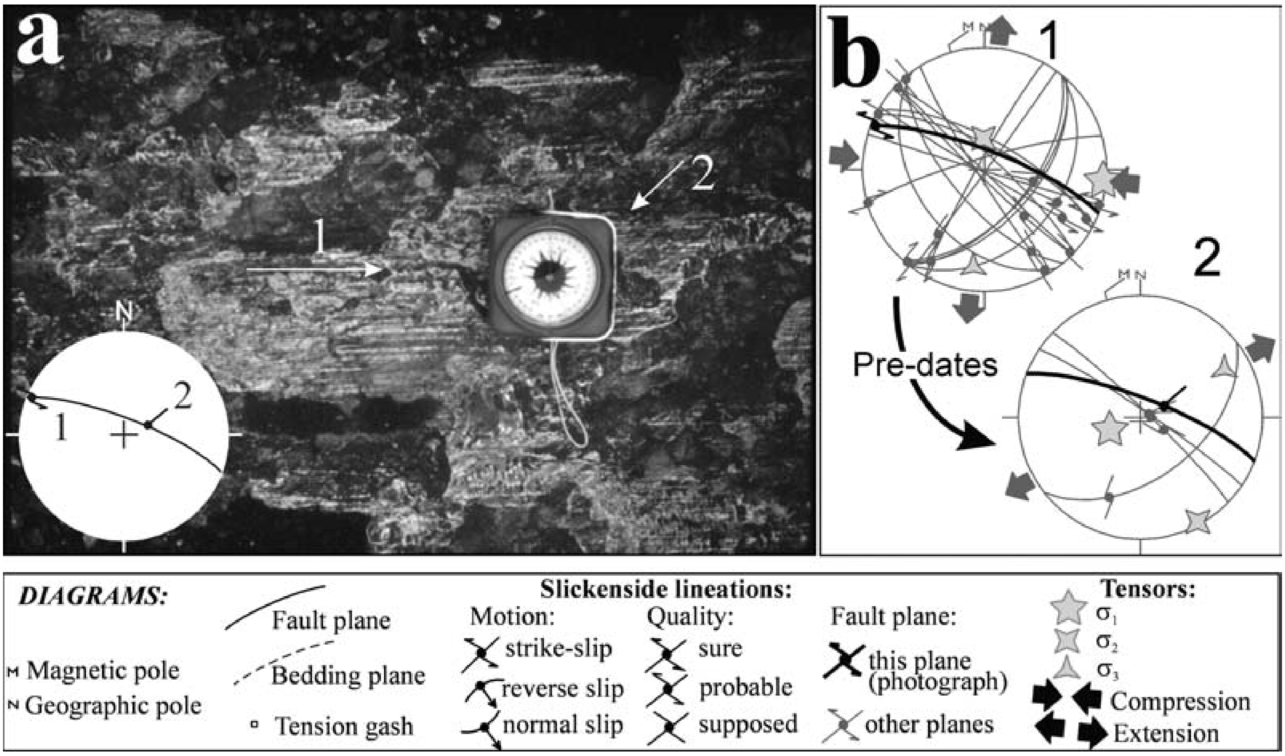

Figure 4. Example of fault slip analysis using the method of Angelier (1984, 1990). (a) Superposition of two generations of striae on a same fault plane at Beaudry quarry (site number 7 on Fig. 2), indicating relative chronology between two supposed distinct events, (b) diagrams showing fault striae measured on this plane (black lines), and other mechanically consistent faults measured in the same site (grey lines), with tensors calculated using the method of Angelier (1984, 1990). Diagrams: Schmidt's lower hemisphere, equal area projection. Size of the compass: 9 cm.

that the stress regime and corresponding orientations of stress axes remained fairly homogeneous throughout the area. This approach has been tested and validated in different geological environments, indicating that local palaeostress reconstructions using minor faults can be extrapolated at a regional scale and yield reliable results (e.g. Angelier, Barrier & Chu, 1986; Pavlides & Montrakis, 1987; Faure, Tremblay & Angelier, 1996; Zanchi & Gritti, 1996).

4.c. Reconstructed palaeostresses

Compilation of field observations of fault striae populations allows the characterization of successive states of stress on a regional scale (Fig. 6). For each analysed site, we commonly measured several stress tensors, but overall, three compressional events (trending WNW, NNW and NE–SW) and three extensional events (trending NW–SE, NNW, and NNE to NE–SW) have been identified (Tables 1, 2, Fig. 6). The regional recurrence and relative homogeneity of these determined stress trends validate the analytical method that has been used, and suggest that fault motions between blocks did not significantly disturb regional stresses. The NW–SE extension has been tied with N040- and N090-trending normal faults. The WNW compression induced or reactivated N090- and N140-trending strike-slip faults, and reactivated some N040-trending faults into reverse faults. A less important NNW compression has induced strike-slip faulting. Extensions trending NE–SW and NNW are characterized by numerous oblique slips (normal-strike-slip), probably because motions occurred on pre-existing faults. These extensions have reactivated N090, N040 and N140 faults with normal and strike-slip motions, and locally led to neoformed N120, N090 and N040 normal faults. Finally, a compression trending NE–SW is characterized by reverse and strike-slip reactivation of older faults (Fig. 6).

Twin measurements were made on sparitic calcite crystals in rock matrix of six samples. Analysed samples display a nearly random crystallographic orientation. In most samples, calcite twins are straight and narrow, indicating twinning at low temperature (<300 °C) and low strain (<2–3 %) (e.g. Groshong, 1974; Friedman & Heard, 1974; P. Laurent, unpub. Ph.D. Thesis, Univ. Montpellier, France, 1984) (Fig. 5). Under such conditions, strain and stress tensors can be considered as nearly coaxial at the sample scale.

The analysis of twinning in calcite samples reveals polyphase deformation. Calculated stress tensors are similar to those reconstructed with fault slip analysis, except for the NW–SE extension, which is never reconstructed. The NE–SW compression is reconstructed in almost all samples.

https://doi.org/10.1017/S0016756803007283 Published online by Cambridge University Press

Table 1. Stress tensors reconstructed by inverse analysis of fault slips

Site	No.	Ch	U	Type	$\sigma 1$	$\sigma 2$	$\sigma 3$	Φ	α	RUP	N
1	1	2/0	Bk	e° NNW	349 65	233 11	**139** 22	0.9	11.9	49	4
Q	2			c° WNW	**302** 03	163 86	**032** 03	0.4	5.5	13	8
	3			c° NE	**222** 02	041 88	**132** 00	0.4	6.5	41	8
2	1		Ch	c° WNW	**294** 10	086 79	**203** 05	0.4	10.8	36	9
Q	2			c° NE ?	**046** 12	164 65	**312** 21	0.6	15.6	48	4
3NE			Ch	e° NE	150 80	287 07	**018** 06	0.4	7.2	54	10
4	1		Ch	c° WNW	**122** 03	327 86	**212** 01	0.5	4.2	38	16
Q	2			c° NE	**201** 03	307 79	**111** 10	0.4	8.9	26	12
5NE			Cr	c° NE	**242** 05	348 70	**150** 19	0.1	15.1	35	11
6	1	5/0	Ch	e° NW	089 78	296 10	**205** 05	0.5	9.4	30	7
Q	2			c° WNW	**124** 07	241 75	**032** 13	0.1	9.1	54	16
	3			e° NNW	073 49	257 41	**165** 02	0.9	14.1	43	15
	4			e° NE	283 78	098 12	**188** 01	0.0	8.7	84	7
7	1	5/1	Pr	e° NW	283 86	048 02	**139** 03	0.5	3.0	12	5
Q	6			c° NE ?	**226** 02	317 29	132 60	0.1	10.0	27	5
	2			c° WNW	**095** 03	358 69	**186** 21	0.3	21.4	46	18
	3			c° NNW	**155** 07	328 83	**064** 01	0.5	14.1	31	9
	4			e° NE	248 68	151 03	**060** 22	0.3	6.5	30	5
	5			e° NNW	152 67	019 16	**284** 16	0.2	7.8	33	5
8NE	1	3/0	Pr	e° NW	283 81	063 07	**153** 06	0.6	10.9	29	11
	2			c° WNW	**102** 07	000 57	**196** 32	0.6	14.5	37	9
	3			e° NNW	031 80	243 08	**152** 05	0.7	19.0	50	7
	4			c° NE	**206** 18	351 68	**112** 12	0.7	18.6	54	10
9NE			Pr	c° NE	**054** 16	147 12	271 70	0.0	12.7	52	13
10	1	1/0	Tt	c° WNW?	**114** 03	239 84	**024** 05	0.6	4.7	41	11
Q	2			c° NE ?	**036** 18	209 71	**306** 02	0.7	5.1	27	4
11	1	1/0	Tt	c° NNW	**162** 01	062 82	**253** 08	0.4	5.4	19	7
Q	2			c° NE	**048** 04	143 51	**314** 39	0.1	6.1	28	5
12	1	1/0	Pr	e° NW	328 74	219 05	**128** 15	0.5	8.1	28	14
Q	2			c° NNW	**156** 06	041 75	**247** 15	0.2	18.3	46	6
13NE			Pr	e° NW	223 76	039 14	**129** 01	0.2	14.3	40	9
14	1	3/0	Ch	c° NE	**071** 05	282 84	**161** 03	0.3	7.4	20	7
Q	2			e° NE	129 42	287 45	**028** 11	0.9	14.9	57	4
15	1	1/0	Tt/Ch	c° WNW	**299** 02	184 84	**029** 05	0.3	7.2	32	8
Q	2			c° NE	**231** 03	136 62	323 28	0.1	5.2	29	8
	3			e° NE	329 56	162 34	**068** 06	0.8	13.2	34	5
16	?	1/0	Ch	c° NE	**016** 16	121 43	271 42	0.1	8.6	39	11
Q	?			e° NNW?	083 70	282 19	**189** 06	0.5	11.0	38	4

Site: see numbers in Fig. 2d (Q: quarry, NE: natural exposure); No.: chronological order (example Fig. 4); Ch: number of chronological observations consistent/inconsistent with order proposed; U: faulted geological unit (Pr: Precambrian, Bk: Beekmantown, Ch: Chazy, Tt: Trenton, Cr: Cretaceous); Type: associated regional state of stress (Fig. 6), c°: compression, e°: extension; $\sigma_1, \sigma_2, \sigma_3$: principal axes of the stress tensor (trend-plunge, in degrees), with directions of compression (σ_1) or extension in bold (σ_3); $\Phi = (\sigma_2 - \sigma_3)/(\sigma_1 - \sigma_3)$; α, RUP: estimators from Angelier's program (1990), see text; N: number of data.

Table 2. Stress tensors reconstructed by inverse analysis of calcite twinning

Site	U	Type	$\sigma 1$	$\sigma 2$	$\sigma 3$	Φ	f	MT	NT	M	N
6A	Ch	c° NE	**220** 03	347 84	**130** 04	0.3	0	56	16	46	100
Q		e° NE?	**150** 18	272 58	**051** 25	0.4	0.06	40	16	35	100
6B	Ch	c° WNW?	**078**.20	343.16	216.65	0.5	0.2	106	70	357	91
		c° NE	**203**.19	299.15	065.65	0.2	0.5	69	58	48	91
15	Tt/Ch	c° NE	**213** 01	303 09	119 81	0.4	0.73	160	61	36	98
Q		c° WNW	**108** 19	236 51	**010** 21	0.4	0.35	105	59	23	93
		e° NE	**160** 15	007 73	**252** 07	0.6	0.15	73	55	15	90
16	Ch	c° NE	**216** 17	117 28	333 56	0.1	0.22	124	41	42	98
Q		e° NNW	**264** 40	059 48	**163** 12	0.3	0.13	72	41	23	93
		e° NE	**148** 38	283 43	**038** 24	0.5	0	46	39	15	95
17	Bk	c° NNW	**172** 35	334 54	**076** 09	0.2	0.08	43	20	37	95
Q		e° NNW	**263** 33	037 47	**156** 24	0.9	0.03	27	20	33	95
18	Pr/Bk	c° WNW	**106**.13	217.58	**009**.29	0.4	0.00	44	14	19	100
Q		c° NE	**003**.06	245.77	**092**.12	0.2	0.09	19	14	18	93

U: sampled geological unit; $\sigma_1, \sigma_2, \sigma_3$, Φ: see Table 1; MT, NT: respectively, total number of twinned and untwinned planes considered for tensor calculation; M, N: respectively, rate of twinned and untwinned planes consistent with the result; f: intra-program function indicating quality of the result (Etchecopar, unpub. Ph.D. Thesis, Univ. Montpellier, France, 1984; see Tourneret & Laurent, 1990).

https://doi.org/10.1017/S0016756803007283 Published online by Cambridge University Press

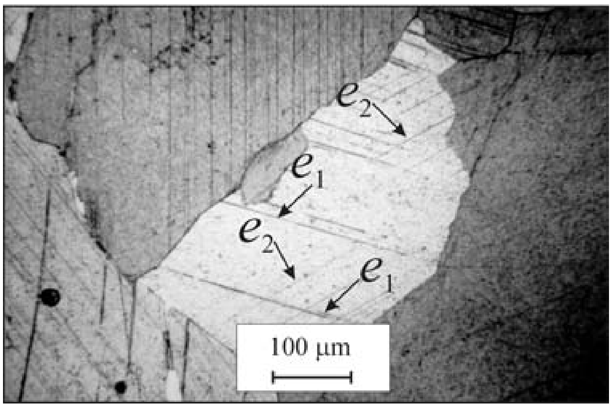

Figure 5. Example of measured mechanical twin sets in calcite. Calcite twins are thin and not curved, indicating low strain at low temperature. Arrows indicate two families (e_1 and e_2) of twin lamellae in one crystal nearly 300 μm in size.

Four samples (6A, 6B, 15, 16, Table 2) were collected in sites where faults were also measured, which provided independent control on palaeostress determinations from both methods. In site 15, stress analyses by calcite twin inversion and by fault slip inversion yielded similar results: NE–SW compression (N051 and N033 for calcite twinning and fault slip data, respectively), WNW compression (N119 and N108), and NE–SW extension (N068 and N072). For site 16, both methods revealed the NE–SW compression (N016 and N036) and the NNW extension (N009 and N156); the analysis of calcite twins revealed, however, a supplementary state of stress (NE–SW extension). For site 6, states of stress reconstructed with fault slip data are not completely reconstructed with the analysis of calcite twins, most probably due to a very low number of calcite twin measurements.

Two samples (17, 18; Table 2) were collected in sites where no macroscopic faults were observed. These samples show polyphase deformation, and the reconstructed stress tensors are consistent with those reconstructed by fault slips in other sites (NNW, WNW and NE–SW compressions, NNW extension). This is consistent with the hypothesis that calcite twinning is more sensitive to stress than faulting, due to the occurrence of higher differential stress during faulting than during calcite twinning (e.g. Rocher *et al.* 1996). Calcite twinning analysis is therefore a useful tool to reconstruct palaeostresses in weakly deformed regions, such as the Montréal area.

4.d. Age constraints on reconstructed tectonic events

Field relationships (e.g. Fig. 4) between the various sets of faults and fractures suggest the following succession of events (Fig. 6): (1) an NW–SE extensional event (Fig. 6a), (2) WNW and NNW compressional events (Fig. 6b,b′), (3) NE–SW, then NNW extensional events (Fig. 6c,c′), and finally (4) a NE–SW compression (Fig. 6d). Such successive stress patterns have also been recognized in the St Lawrence Lowlands and the Appalachian Belt (Gélard, Jébrak & Prichonnet, 1992; S. Faure, unpub. Ph.D. thesis, Univ. du Québec, 1995; Rocher *et al.* 2000*b*; Rocher & Tremblay, 2001).

The fact that the NW–SE extension is not reconstructed with calcite twinning and that the NE–SW compression is reconstructed in nearly all samples indicates that the NW–SE extension occurred before the first calcite crystallization, and that the NE–SW compression occurred after the last crystallization, thus partially confirming the relative chronology established with field observations.

N090-trending faults cross-cut the NE–SW fold axes in the region of study. These minor folds are related to the Chambly–Fortierville syncline system (Figs 2d, 3b) and can be considered as post-Taconian or post-Acadian in age (Table 3). Structural relationships between these faults and the Monteregian intrusions also suggest that they represent crustal fractures that were reactivated during or after the Early Cretaceous magmatism (e.g. McHone, 1978; Bédard, 1985; McHone, Ross & Greenough, 1987; Faure, Tremblay & Angelier, 1995). We thus used these N090-trending faults as a time marker, and they correspond, on the basis of palaeostress reconstruction, to a period of significant extension trending nearly N–S (NE–SW to NNE, and NNW; Fig. 6c,c′). Field relationships among faults and fractures in the area indicate that these N090-trending faults were formed after a period of compressions trending WNW–ESE and NNW, which could be correlated with Appalachian orogenies. The WNW–ESE compression is probably related to the Taconian and/or the Acadian orogenies (Faure, Tremblay & Angelier, 1995, 1996), whereas NNW compression is possibly related to the Alleghanian orogeny, which is not structurally significant in Québec but has been recognized by palaeostress reconstructions by Faure, Tremblay & Angelier (1996). We conclude that N090-trending faults and the associated N–S extensions have occurred between Permian and Early Cretaceous times. This possibly corresponds to the 160–140 Ma tectonothermal event proposed by Glasmacher, Tremblay & Zentilly (1998) on the basis of apatite fission track dating of a N040 brittle fault in the Québec city area (Montmorency fault, Fig. 1b), which has been tentatively attributed to the collapse of the Laurentian margin during the opening of the Atlantic Ocean (Table 3). Fault slip data from the Montréal area are indicative of two phases of extension trending nearly N–S: (1) a NNE to NE–SW extension (Fig. 6c) associated with normal faulting along N120-trending faults and along some N090-trending faults, and (2) a NNW extension (Fig. 6c′) mainly associated with N090-trending normal to left-lateral strike-slip faults (which locally cross-cut the N120-trending faults; Fig. 3b), and with N040-trending faults. The N090-trending faults affect the Oka and St-André Cretaceous

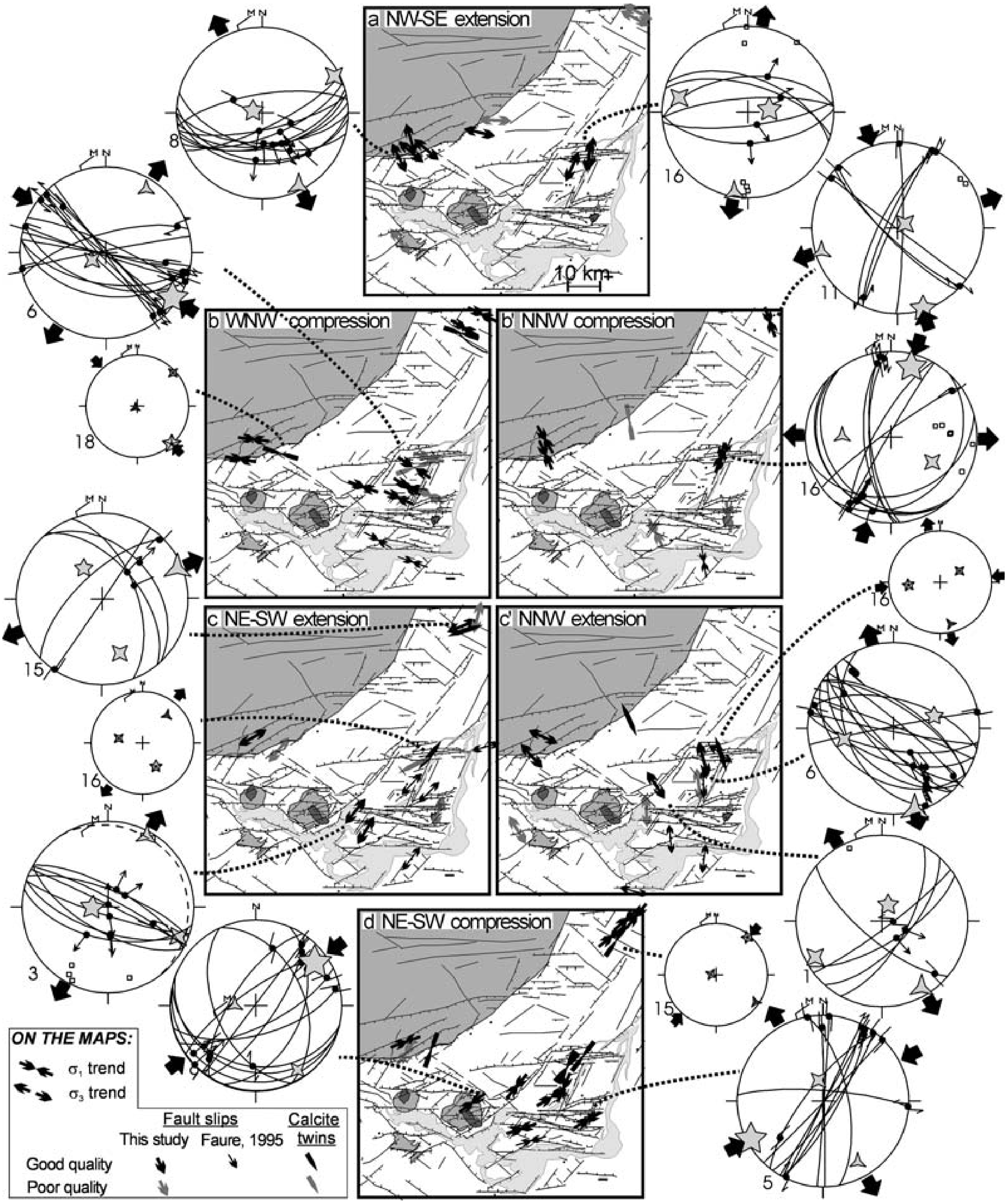

Figure 6. Successive tectonic events reconstructed by inverse analyses of fault slips and of calcite twins, from localities shown in Figure 2. See also Figure 2 legend. (a) NW–SE extension that we attribute to Iapetus rifting and/or to syn-orogenic subsidence; (b,b′) WNW and NNW compressions due to Appalachian orogeny; (c,c′) NE–SW and NNW extensions interpreted as related to the Mesozoic opening of the North Atlantic Ocean; (d) NE–SW compression probably resulting from the push of the North Atlantic spreading ridge on the North American Plate (S. Faure, unpub. Ph.D. thesis, Univ. du Québec, 1995). The small and large diagrams (see legend in Fig. 4) represent examples of tensor axes reconstructed respectively with calcite twins and fault slips, with site number (see Tables 2 and 1, respectively).

https://doi.org/10.1017/S0016756803007283 Published online by Cambridge University Press

Table 3. Relative and absolute dating of structures

Major structures	Normal faults N040	N120	N090	Ages
Iapetus rifting; subduction	+	+	+	Late Precambrian–Early Cambrian
Appalachian NE-trending folds and thrusts	∗			Late Ordovician–Devonian–Permian
”		+		?
Major collapse			+	160–140 Ma
Cretaceous intrusions			+	125 Ma
”	+		+	?
”	+			?

+: faults activated.
∗: N040 border faults could have been locally inverted and then activated as normal faults during Appalachian collision and subsidence of the foreland basin.

intrusions. These extensions can be considered to be the result of a single and incremental extension, the Mesozoic opening of the North Atlantic Ocean.

The observed cross-cutting relationships and geodynamic constraints inferred for the Laurentian margin and the Appalachian orogen (e.g. Williams, 1979; St-Julien & Hubert, 1975) indicate the existence of an extensional event older than Appalachian compressions (WNW and NNW compressions), that is currently attributed to Iapetus rifting (e.g. Kumarapeli, 1985). According to Lavoie (1994), Salad Hersi & Lavoie (1999) and Salad Hersi & Dix (1999), erosional unconformities in the St Lawrence Lowlands platform and regional variation in depositional facies and thickness of foreland basin limestone units can be attributed to syn-sedimentary faulting due to syn-orogenic subsidence, and are also consistent with a phase of normal faulting. In the Montréal area, this early event is expressed as a NW–SE extension related to N040- and N090-trending normal faults. These faults commonly show evidence for reactivation as reverse and strike-slip faults during Appalachian compressions (Figs 4, 6b,b′), and as normal faults during the Mesozoic (Fig. 6c,c′). This early phase of normal faulting has also been recognized in other areas of the St Lawrence Lowlands; it affects rock units which vary between Precambrian and Middle–Late Ordovician (deposition of Chazy, Black River and Trenton formations), but does not affect younger rocks where exposed (Utica and Sainte-Rosalie formations: see, e.g. Québec city area, Rocher & Tremblay, 2001), which indicate that the major part of this extension occurred before the end of the Ordovician. It can be concluded that some of the N040- and N090-trending normal faults of southwestern Québec are pre- to syn-Taconian (Late Ordovician) and could partially result from Iapetus rifting, but also from the collapse of the Laurentian margin due to syn-orogenic flexure caused by subduction plate stretching.

Finally, we recognized a late NE–SW compression, which occurred after the emplacement of the Monteregian intrusions (because faults related to that event affect the Mont Royal pluton; Fig. 6d, site 5 in Table 1). This event is most probably related to the Tertiary to present-day regional state of stress of eastern North America, which has been attributed to the push of the North Atlantic spreading ridge on the North American Plate (Zoback *et al*. 1986).

5. Structural implications for the Montréal area

Palaeostress reconstructions and field relationships of the various generations of supracrustal faults are used to infer which set of regional faults was most likely formed, or reactivated during each tectonic event. An example of field relationships that can be used for this purpose is given by faults observed at the Pointe-des-Carrières (site 3, Fig. 2c), where abundant minor normal faults trending nearly N110, and which are consistent with NE–SW extension (Fig. 6c), suggest the activation of the nearby N110-trending Ile Bizard fault (Fig. 3b) during this event (Fig. 7d). Using this type of structural information and on the basis of age constraints for each fault set, we propose a tentative structural evolution for the Montréal area (Fig. 7).

The initial NW–SE extension (Fig. 7a) is attributed to the opening of the Iapetus Ocean and to the subsequent development of the Laurentian continental margin. It is responsible for the present-day shape of the St Lawrence Lowlands. It has generated N040-trending faults bordering the St Lawrence Lowlands to the northwest, and N090-trending faults occurring in the northern part of Montréal Island and in the vicinity of Mont Rigaud (Fig. 2c).These faults are locally associated with rift-related intrusions and dykes. No outcrop allowed us to determine whether or not some of the N120-trending faults related to the Ottawa-Bonnechère graben were formed during that event (labelled with question marks on Fig. 7a).

The subsequent Appalachian phase of regional deformation corresponds to a WNW compression (Fig. 7b) and then to a minor NNW compression (Fig. 7b′). In Figure 7, we roughly sketched some of the faults activated during these compressional events.

The WNW compression (Fig. 7b) trends N110 to N120, which is almost perpendicular to the Appalachians thrust front (Logan's Line) east of the Montréal area. In the Québec city area (Rocher & Tremblay, 2001), the same compressional event trends N120 to N140, an orientation that is, as in the Montréal region, approximately perpendicular to Logan's Line. Such systematic variations in the orientation of the WNW compression suggest that it is likely related to the main phase of Appalachian thrusting, and that it is characterized by a fan-shaped distribution of compression axes in southern Québec. In the Montréal area, the WNW compression is responsible for folds with NNE-trending axes, and probably for the reactivation of some N090-trending faults into

https://doi.org/10.1017/S0016756803007283 Published online by Cambridge University Press

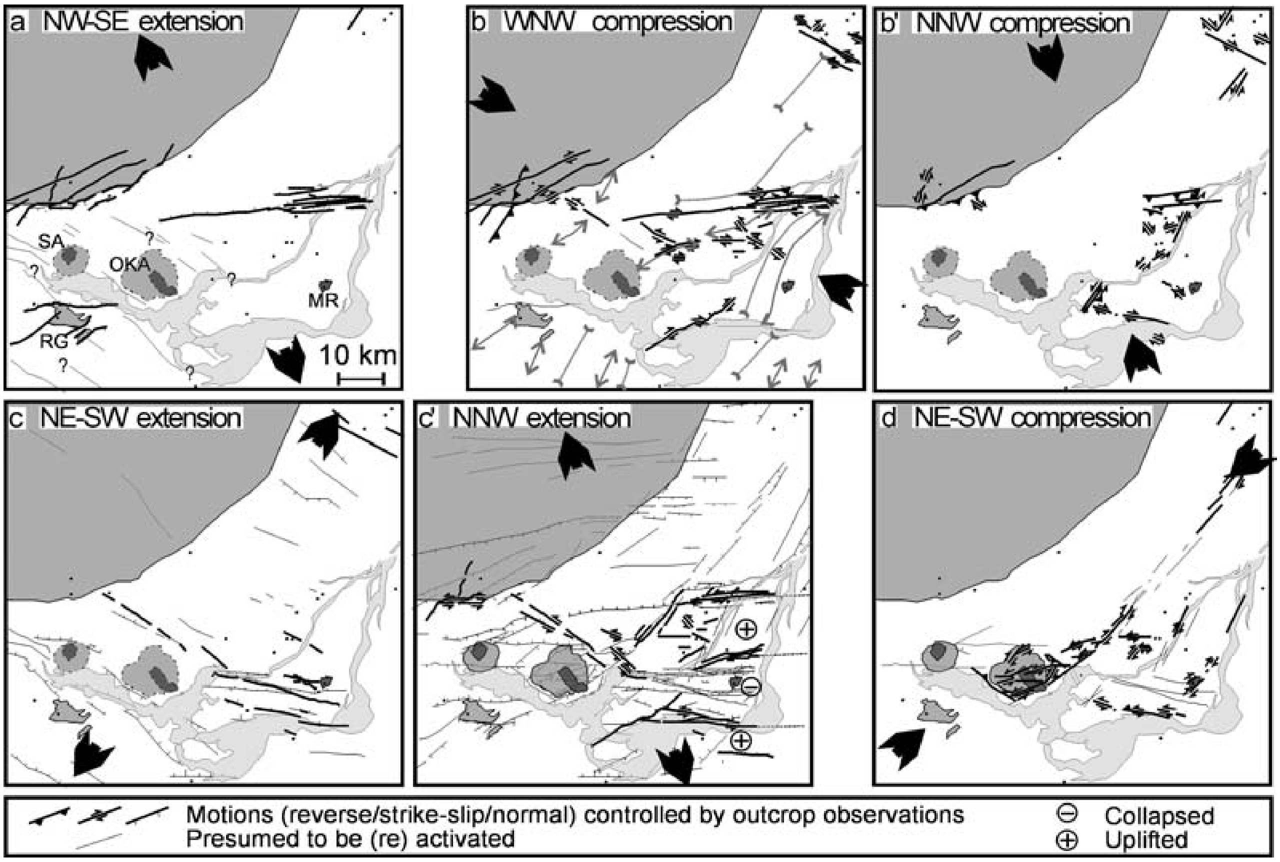

Figure 7. Preliminary structural sketches (represented on present-day structural map) for each reconstructed tectonic event deduced from local palaeostress reconstructions (Fig. 6). Legend and abbreviations as in Figure 2. In (a) to (c) the Monteregians are shown by dashed lines, because they probably did not exist.

strike-slip right-lateral faults, thus behaving as transfer faults. Some of the pre-existing normal faults trending N040–070 and N120 were reactivated as reverse to strike-slip faults.

The NNW compression (Fig. 7b) is mainly responsible for strike-slip conjugate faults trending NW–SE and NNE.

The subsequent phase of faulting is attributed to the opening of the Atlantic–Labrador oceans, and is consistent with the reconstructed extensions trending NE–SW (Fig. 7c) and NNW (Fig. 7c′).

The NE–SW extension (Fig. 7c) is expressed by two sets of N120-trending normal faults that form a small-scale graben (reactivation of the Ottawa–Bonnechère graben?). The first set dips to the north and runs between Mont Rigaud and Oka Hill, and the other set dips to the south and is located to the north of Oka Hill.

The NNW extension corresponds to major N090 normal faults that cross-cut Appalachian folds on Montréal Island (Fig. 7c′). This phase of extension is responsible for the formation of the horst-and-graben geometry of Montréal and Jésus islands. The N090 major faults probably also exist in the eastern part of the Montreal region. The vertical motion along these faults explains the present-day ‘divided’ shape of the Chambly–Fortierville syncline (see Fig. 1); the activity of these faults during the NNW extension would have also raised the syncline (as the North Montréal Island horst). This extension probably ended with the emplacement of Cretaceous intrusions (as suggested by cross-cutting relationships between plutons and N090-trending faults; see Section 3.b and Table 3). It also reactivated the N040 border faults of the St Lawrence Lowlands with normal slip motion, as well as some pre-existing N120-trending faults with normal to left-lateral strike-slip motions. Such reactivation of sub-vertical faults may have induced important fault offsets, while dry friction along brittle fault planes allowed the formation of pseudo-tachylyte.

Finally, a NE–SW compression (Fig. 7d) post-dating these events was associated with the formation of strike-slip faults that cross-cut the Monteregian intrusions.

6. Conclusions

The Montréal region offers the opportunity to study an area which has undergone a complete Wilson tectonic cycle (Wilson, 1966). Its tectonic analysis required the combination of palaeostress reconstructions with two independent methods, and various types of structural investigations. It allowed us to propose a tectonic evolution for the St Lawrence Lowlands in the Montréal area. Preliminary studies near Québec city and Trois-Rivières (Rocher & Tremblay, 2001; Rocher *et al.* 2000*b*) and in the Charlevoix area (Lemieux, Tremblay & Lavoie, 2000; Tremblay & Lemieux, 2001) show results similar to those obtained during this study. However, age constraints are few and the precise dating of faulting events (apatite fission tracks and Ar–Ar studies in progress) would greatly improve the results. The study in the Montréal region reveals the importance of structural inheritance in areas characterized by multiple events of continental rifting and/or intraplate extensional faulting. Our main conclusion is that some of the NW–SE extension and associated N040 and N090 normal faults in the Montréal area are related to the opening of the Iapetus Ocean and/or to the syn-orogenic plate flexuring during the Appalachian orogeny. However, we speculate that the major collapse event along these faults is likely related to the post-Appalachian NE–SW and NNW distensions, caused by the opening of the North Atlantic–Labrador Sea in Mesozoic times. The pre-existence of N040-trending subvertical basement faults before the approximately N–S-trending Mesozoic extensions can explain the predominance of oblique slips on several fault families, the fault offsets of hundreds of metres near Montréal, and the overall NE–SW orientation of the St Lawrence Lowlands.

Acknowledgements. This study has been supported by the Geological Survey of Canada (Appalachian Foreland and Platform NATMAP project 99001), the Institut National de la Recherche Scientifique (INRS post-doctoral grant to M. Rocher), and by the Natural Sciences and Engineering Research Council (NSERC) of Canada (PG-105669 to A. Tremblay). Geological data from the Montréal Island was compiled with the help of the 'Ville de Montréal'. We thank R. Lisle and M. Jébrak for critical comments, A. Fortin for his active collaboration in the field, and the hydrogeological team of the Québec Geoscience Centre (QGC) project for its welcome at Oka during the summer of 2000.

References

ANGELIER, J. 1975. Sur l'analyse de mesures recueillies dans des sites faillés: l'utilité d'une confrontation entre les méthodes dynamiques et cinématiques. *Comptes-Rendus de l'Académie des Sciences* (D) **281**, 1805–8.

ANGELIER, J. 1976. Sur l'analyse de mesures recueillies dans des sites faillés: l'utilité d'une confrontation entre les méthodes dynamiques et cinématiques: erratum. *Comptes-Rendus de l'Académie des Sciences* **283**, 466.

ANGELIER, J. 1984. Tectonic analysis of fault slip data sets. *Journal of Geophysical Research* **89**, 5835–48.

ANGELIER, J. 1990. Inversion of field data in fault tectonics to obtain the regional stress. III: A new rapid direct inversion method by analytical means. *Geophysical Journal International* **103**, 363–76.

ANGELIER, J., BARRIER, E. & CHU, H. T. 1986. Plate collision and paleostress trajectories in a fold-thrust belt; the Foothills of Taiwan. *Tectonophysics* **125**, 161–78.

BÉDARD, J. H. 1985. The opening of the Atlantic, the Mesozoic New England igneous province, and mechanisms of continental breakup. *Tectonophysics* **113**, 209–32.

CAREY, E. & BRUNIER, B. 1974. Analyse théorique et numérique d'un modèle mécanique élémentaire appliqué à l'étude d'une population de failles. *Comptes-Rendus de l'Académie des Sciences* (D) **279**, 891–4.

CARIGNAN, J., GARIÉPI, C. & HILLAIRE-MARCEL, C. 1997. Hydrothermal fluids during Mesozoic reactivation of the St. Lawrence rift system, Canada: C, O, Sr and Pb isotopic characterization. *Chemical Geology* **137**, 1–21.

CLARK, T. H. 1940. Rapport préliminaire, région de Montréal. *Service des Mines, Québec*, R. P. **147**.

CLARK, T. H. 1941. Rapport préliminaire sur la région de Montréal. *Service des Mines, Québec*, R. P. **158**.

CLARK, T. H. 1947. Rapport sommaire sur les Basses Terres au sud du Saint-Laurent. *Ministère des Mines, Québec*, R. P. **204**.

CLARK, T. H. 1972. Montreal area. *Ministère des Richesses Naturelles du Québec, Geological Report* **152**, 244 pp.

DEFFONTAINES, B. 1990. *Développement d'une méthodologie d'analyse morphostructurale et morphotectonique. Analyse des surfaces enveloppes du réseau hydrographique et modèles numériques de terrain. Applications au NE de la France.* Philosophiae Doctor Thesis, Univ. P. et M. Curie, Rapport BRGM 32005, 194 pp.

DEFFONTAINES, B. & CHOROWICZ, J. 1991. Principles of drainage basin analysis from multisource data: application to the structural analysis of the Zaire Basin. *Tectonophysics* **194**, 237–263.

DIETRICH, D. & SONG, H. 1984. Calcite fabrics in a natural shear environment, the Helvetic nappes of western Switzerland. *Journal of Structural Geology* **6**, 19–32.

DOIG, R. & BARTON, J. M. 1968. Ages of carbonatites and other alkaline rocks in Quebec. *Canadian Journal of Earth Sciences* **5**, 1401.

ETCHECOPAR, A., VASSEUR, G. & DAIGNIERES, M. 1981. An inverse problem in microtectonics for the determination of stress tensor from fault striation analysis. *Journal of Structural Geology* **3**, 51–65.

FAURE, S., TREMBLAY, A. & ANGELIER, J. 1995. State of intraplate stress and tectonism of northeastern America since Cretaceous times, with particular emphasis on the New England–Quebec igneous province. *Tectonophysics* **255**, 111–34.

FAURE, S., TREMBLAY, A. & ANGELIER, J. 1996. Alleghanian paleostress reconstruction in the northern Appalachian: intraplate deformation between Laurentia and Gondwana. *Geological Society of America Bulletin* **108**, 1467–80.

FOLAND, K. A., GILBERT, L. A., SEBRING, C. A. & JIANG-FENG, C. 1986. $^{40}Ar/^{39}Ar$ ages for plutons of the Monteregian hills, Quebec: Evidence for a single episode of Cretaceous magmatism. *Geological Society of America Bulletin* **97**, 966–74.

FRIEDMAN, M. & HEARD, H. C. 1974. Principal stress ratios in Cretaceous limestones from Texas Gulf Coast. *American Association of Petroleum Geologists Bulletin* **58**, 71–8.

GÉLARD, J. P., JÉBRAK, M. & PRICHONNET, G. 1992. Les contraintes phanérozoïques dans la plate-forme du Saint-Laurent, région de Montréal, Québec. *Canadian Journal of Earth Sciences* **29**, 499–505.

GITTINS, J. R., MCINTYRE, M. & YORK, D. 1967. The ages of carbonatite complexes in eastern Canada. *Canadian Journal of Earth Sciences* **4**, 651–5.

GLASMACHER, U., TREMBLAY, A. & ZENTILLY, M. 1998. Post-Triassic thermo-tectonic evolution of the Laurentian margin in Quebec, Canada. *GAC-MAC meeting, Québec, Abstract volume* A-**66**.

GLOBENSKY, Y. 1987. Géologie des Basses-Terres du Saint-Laurent. *Ministère de l'Energie et des Ressources du Québec* MM**85–02**, 63 pp.

GROSHONG, R. H. 1974. Experimental test of least-squares strain gauge calculation using twinned calcite. *Geological Society of America Bulletin* **85**, 1855–64.

KAMO, S. L. & KROGH, T. E. 1995. Chicxulub crater source for shocked zircon crystals from the Cretaceous–Tertiary boundary layer, Saskatchewan: evidence from new U–Pb data. *Geology* **23**, 281–4.

KNIGHT, I., JAMES, N. P. & LANE, T. E. 1991. The Ordovician St. George Unconformity, northern Appalachians: the relationship of plate convergence at the St. Lawrence Promontory to the Sauk/Tippecanoe sequence boundary. *Geological Society of America Bulletin* **103**, 1200–25.

KUMARAPELI, P. S. 1985. Vestiges of Iapetan rifting in the craton West of the Northern Appalachians. *Geoscience Canada* **12**, 54–9.

KUMARAPELI, P. S. & SAULL, V. A. 1966. The St. Lawrence valley system: a North american equivalent of the East African rift valley system. *Canadian Journal of Earth Sciences* **3**, 639–58.

LACOMBE, O., ANGELIER, J., BERGERAT, F., LAURENT, P. & TOURNERET, C. 1990. Joint analyses of calcite twins and fault slips as a key for deciphering polyphase tectonics: Burgundy as a case study. *Tectonophysics* **182**, 279–300.

LACOMBE, O., ANGELIER, J. & LAURENT, P. 1992. Determining paleostress orientations from faults and calcite twins: a case study near the Sainte-Victoire Range. *Tectonophysics* **201**, 141–56.

LACOMBE, O., ANGELIER, J., ROCHER, M., BERGUES, J., DEFFONTAINES, B., CHU, H.-T., HU, J.-C. & LEE, J.-C. 1996. Contraintes et plissement au front d'une chaîne de collision: l'exemple des calcaires récifaux pliocènes de Yutengping (Taiwan). *Bulletin de la Société Géologique de France* **167**, 361–74.

LAVOIE, D. 1994. Diachronous tectonic collapse of the Ordovician continental margin, eastern Canada: comparison between the Quebec Reentrant and St. Lawrence Promontory. *Canadian Journal of Earth Sciences* **31**, 1309–19.

LAVOIE, D. 1995. A Late-Ordovician high-energy temperate-water carbonate ramp, southern Québec, Canada: implications for Late Ordovician Oceanography. *Sedimentology* **42**, 95–116.

LEMIEUX, Y., TREMBLAY, A. & LAVOIE, D. 2000. Stratigraphy and structure of the St. Lawrence Lowland in the Charlevoix area, Quebec: relationships to impact cratering. *Current Research* **2000-D2**, Commission Géologique du Canada, Ottawa, 7 pp.

MCHONE, J. G. 1978. Distribution, orientations and ages of mafic dikes in central New England. *Geological Society of America Bulletin* **89**, 1645–65.

MCHONE, J. G. & BUTLER, J. R. 1984. Mesozoic igneous provinces of New England and the opening of North Atlantic Ocean. *Geological Society of America Bulletin* **95**, 757–65.

MCHONE, J. G., ROSS, M. E. & GREENOUGH, J. D. 1987. Mesozoic dyke swarms of eastern North America. In *Mafic Dyke Swarms* (eds H. C. Halla and W. F. Fahrig), pp. 279–88. Canadian Special Paper no. 34, Geological Association.

PAVLIDES, S. & MONTRAKIS, D. 1987. Extensional tectonics of northwestern Macedonia, Greece, since the Late Miocene. *Journal of Structural Geology* **9**, 385–92.

PE-PIPER, G. & JANSA, L. F. 1987. Geochemistry of Late Middle Jurassic–Early Cretaceous igneous rocks on the eastern North American margin. *Geological Society of America Bulletin* **99**, 803–13.

PFIFFNER, O. A. & BURKHARD, M. 1987. Determination of paleostress axes orientations from fault, twin and earthquake data. *Annales Tectonicae* **1**, 48–57.

PHILPOTTS, A. R. 1974. The Monteregian province. In *The alkaline rocks* (ed. H. Sorenson), pp. 293–310. New York: Wiley and Sons.

ROCHER, M., LACOMBE, O., ANGELIER, J. & CHEN, R. W. 1996. Mechanical twin sets in calcite as markers of recent collisional events in a fold-and-thrust belt: evidence from the reefal limestones of southwestern Taiwan. *Tectonics* **15**, 984–96.

ROCHER, M., LACOMBE, O., ANGELIER, J., DEFFONTAINES, B. & VERDIER, F. 2000*a*. Cenozoic faulting and folding in the North Pyrenean foreland (Aquitaine Basin, France): insights from paleostress reconstructions. *Journal of Structural Geology* **22**, 627–45.

ROCHER, M., TREMBLAY, A., NADEAU, L. & LAVOIE, D. 2000*b*. Analyse structurale et tectonique des Basses-Terres du Saint-Laurent: résultats préliminaires. *Current Research* **2000-D12**, Commission Géologique du Canada, Ottawa, 7 pp.

ROCHER, M. & TREMBLAY, A. 2001. L'effondrement de la plate-forme du Saint-Laurent: ouverture de Iapetus ou de l'Atlantique? Apport de la reconstitution des paléocontraintes dans la région de la ville de Québec (Canada). *Comptes-Rendus de l'Académie des Sciences* (D) **333**, 171–8.

ROSS, M., PARENT, M., BOLDUC, A. M., HUNTER, J. A. & BENJUMEA, B. 2001. Etude preliminaire des formations quaternaires comblant les vallées des Basses Laurentides, nord-ouest de Montréal, Québec. *Current Research* **2001-D5**, Commission Géologique du Canada, Ottawa, 19 pp.

SALAD HERSI, O. & DIX, G. R. 1999. Blackriveran (Lower Mohawkian, Upper Ordovician) lithostratigraphy, rythmicity, and paleogeography: Ottawa embayment, eastern Ontario, Canada. *Canadian Journal of Earth Sciences* **36**, 2033–50.

SALAD HERSI, O. & LAVOIE, D. 1999. Paleogeographic reconstruction of the Quebec reentrant, Central St. Lawrence platform; southwestern Quebec–eastern Ontario, Canada. *GAC-MAC Annual Meeting, Sudbury, Ontario, Abstract volume* **107**.

SALAD HERSI, O. & LAVOIE, D. 2000*a*. Pre-Cairnside Formation carbonate-rich sandstone: evidence for a Cambrian carbonate platform in southwestern Quebec. *Current Research* **2000-D3**, Commission Géologique du Canada, Ottawa, 8 pp.

SALAD HERSI, O. & LAVOIE, D. 2000*b*. Lithostratigraphic revision of the Upper Cambrian Cairnside Formation, Upper Potsdam Group, southwestern Québec, Canada. *Current Research* **2000-D3**, Commission Géologique du Canada, Ottawa, 8 pp.

SANDFORD, B. U. 1993. Geology of the St. Lawrence Lowland Platform. In *Sedimentary cover of the craton in Canada*,

https://doi.org/10.1017/S0016756803007283 Published online by Cambridge University Press

Chapter II (eds D. F. Stott and J. D. Aitken). Geological Survey of Canada, Geology of Canada 5.
SCANVIC, J. Y. 1983. Utilisation de la télédétection dans les Sciences de la Terre, Manuels et méthodes. *Bureau de Recherche Géologique et Minière* **7**, 159 pp.
SLOSS, L. L. 1988. Forty years of sequence stratigraphy. *Geological Society of America Bulletin* **100**, 1661–5.
ST-JULIEN, P. & HUBERT, C. 1975. Evolution of the Taconian Orogen in the Quebec Appalachians. *American Journal of Science* **275-A**, 337–62.
TOURNERET, C. & LAURENT, P. 1990. Paleostress orientations from calcite twins in the north Pyrenean foreland, determined by the Etchecopar inverse method. *Tectonophysics* **180**, 287–302.
TREMBLAY, A. & LEMIEUX, Y. 2001. Supracrustal faults of the St. Lawrence rift system between Cap-Tourmente and Baie St-Paul, Québec. *Current Research* **2001-D15**, Commission Géologique du Canada, Ottawa, 8 pp.
TURNER, F. J. 1953. Nature and dynamic interpretation of deformation lamellae in calcite of three marbles. *American Journal of Sciences* **251**, 276–98.
TURNER, F. J., GRIGGS, D. T. & HEARD, H. 1954. Experimental deformation of calcite crystals. *Geological Society of America Bulletin* **65**, 883–934.
WILLIAMS, H. 1979. Appalachian orogen in Canada. *Canadian Journal of Earth Sciences* **16**, 797–807.
WILSON, J. T. 1966. Did the Atlantic close and re-open? *Nature (London)* **211**, 676–81.
ZANCHI, A. & GRITTI, D. 1996. Multistage structural evolution of Northern Karakorum (Hunza region, Pakistan). *Tectonophysics* **260**, 145–65.
ZOBACK, M. L., NISHENKO, S. P., RICHARDSON, R. M., HASEGAWA, H. S. & ZOBACK, M. D. 1986. Mid-plate stress, deformation, and seismicity. In *The Western North Atlantic Region* (eds P. R. Vogt and B. E. Tuckolke), pp. 297–312. The Geology of America, vol. M. Boulder: Geological Society of America.